Supplemental Information for

Observing Lysozyme Closing and Opening Motions by

High-Resolution Single Molecule Enzymology

Maxim V. Akhterov[1], Yongki Choi[1], Tivoli J. Olsen[2], Patrick C. Sims[1], Mariam Iftikhar[2],

O. Tolga Gul[1], Brad L. Corso[1], Gregory A. Weiss[2,3*], and Philip G. Collins[1*]

Departments of [1]Physics and Astronomy, [2]Chemistry, and [3]Molecular Biology and Biochemistry,

University of California Irvine, Irvine, California 92697, U.S.A.

A. Materials and Methods

A-1. Lysozyme mutagenesis.

A single-cysteine variant of T4 lysozyme was designed for attachment to SWNT FET devices. The variant was based upon a pseudo-wild-type variant with the substitutions C54T C97A (a generous gift from Prof. Brian Matthews, University of Oregon) that had been previously studied. An ORF encoding this lysozyme variant with the additional mutation S90C provided a template for splice overlap extension PCR. An amplicon encoding the S90C lysozyme variant was subcloned into the pET28 vector for protein overexpression.

A-2. Lysozyme expression and purification.

The pET28-S90C lysozyme plasmid was transformed into BL21 DE3 *E. coli* cells. Transformed cells were spread on agar plates supplemented with kanamycin (40 μg/ml), and were incubated overnight at 37 °C. A single transformant was next used to inoculate 10 ml LB supplemented with kanamycin (40 μg/ml). The culture (10 ml) was used to inoculate 1 L of LB media. Cells were grown at 37 °C to an OD_{600} of 0.8, and induced with 1 mM IPTG. Following induction, the culture was grown at 30 °C for 4 h.

After expression, the culture was centrifuged at 6 krpm (4032 g) for 25 min at 4 °C, and the supernatant decanted. The cell pellet was resuspended in lysis buffer (20 mM Tris, 10 mM NaCl, pH 7.5) before cell lysis by sonication. The resultant cell culture was centrifuged at 16 krpm (17203 g) for 45 min at 4 °C. Subsequently, the supernatant was decanted and filtered (0.45 μm). Next, the cell lysate was applied to a cation exchange column on a BioLogic DuoFlow FPLC. The purified lysozyme fractions were concentrated, filtered (0.45 μM, Millipore), and applied to a Superdex size-exclusion column. The S90C variant of lysozyme was eluted in PBS buffer (138 mM NaCl, 2.7 mM KCl, 8.1 mM Na_2HPO_4, 1.5 mM KH_2PO_4, pH 7.5). The homogeneity of lysozyme variants used in the electronic measurements was >95%, as estimated by SDS PAGE.

A-3. Lysozyme substrate.

Peptidoglycan from *Micrococcus luteus* was purchased from Sigma-Aldrich (St. Louis, MO) and used without further purification as a substrate to assay lysozyme activity (*1*). The

substrate was suspended in PBS (pH 7.5) to a final concentration of 25 μg/ml. Typical experiments flushed the apparatus with 2 mL of substrate supernatant solution to insure the presence of excess substrate in the vicinity of the lysozyme-SWNT device.

A-4. SWNT synthesis and device fabrication.

SWNTs were grown on 4" Si wafers by chemical vapor deposition (CVD) using a monodisperse nanoparticle $Fe_{30}Mo_{84}$ as the catalytic seed (*2*). Nanoparticles were diluted 1:1000 in ethanol and then spin-coated onto a clean wafer surface at 150 rpm. SWNT growth proceeded by a three-step CVD process. The catalyst-coated wafer was oxidized in air at 700 °C, then reduced at 940 °C (520 sccm H_2 in 3000 sccm Ar), and finally exposed to a carbon source at 940 °C (1000 sccm CH_4 + 520 sccm H_2 in 3000 sccm Ar). After CVD synthesis, SWNTs randomly coated the entire wafer at an areal density of approximately 0.01 μm^{-2}. SWNTs were characterized by noncontact atomic force microscopy (AFM, Pacific Nanotechnology Nano-R) and by scanning electron microscopy (SEM, JEOL 6060 at 1 kV). This CVD growth protocol yielded SWNTs with a diameter range of 1.1 - 1.6 nm.

After CVD synthesis, Pd electrodes (30 nm) with a Cr sticking layer (1 nm) were deposited on top of the SWNTs using wafer-scale optical lithography. Source and drain electrodes were separated by 2 μm. An undercut bilayer resist (S1808 on top of LOR-A1, MicroChem) was used for clean liftoff. The p^{++} Si wafer, separated from the SWNT by a 500 thermal oxide, defined a back-gate electrode. Individual devices were electrically probed to identify semiconducting SWNT devices for further use. AFM was used to confirm that only one SWNT formed each source-drain connection.

After initial characterization, each device underwent electrode passivation followed by electron beam lithography. Devices were coated with an electron beam resist (A3 PMMA, MicroChem) and then patterned with an electron beam to expose the middle portion of SWNT channel. This patterning was designed to protect the majority of the surface, especially source and drain electrodes, from contacting the test solutions. After e-beam lithography, devices were re-imaged by AFM to confirm that a ~1.0 μm portion of the SWNT channel was properly exposed and that it remained free of particulates. Similar methods have been described in previous publications (*3, 4*).

A-5. Protein conjugation.

Individual lysozyme molecules were conjugated to SWNT devices using the bifunctional linker molecule *N*-(1-pyrenyl)maleimide (Sigma-Aldrich). The pyrene functionality adhered strongly to SWNT sidewalls via π-π stacking (*5*). The maleimide group formed a stable thioether bond with the single free thiol on the surface of lysozyme. As described above, we expressed a lysozyme variant that only contained a single surface cysteine, resulting in reproducible attachment orientations between different devices. Devices were soaked in a 1 mM solution of pyrene-maleimide in ethanol for 30 min without agitation. Afterwards, excess pyrene-maleimid was removed by rinsing the devices for 5 minutes with 0.1% Tween-20 (Acros Organics) in ethanol and 5 minutes in de-ionized water.

Finally, devices were soaked in a lysozyme solution (54 μM in PBS) for 120 min without agitation. The devices were then rinsed with wash buffer (5 mM KCl, 10 mM Na_2HPO_4, 0.05% Tween-20, pH 7) to remove non-specifically adsorbed lysozyme. Following conjugation, devices were either used for measurements or stored in PBS. As stated in the manuscript,

devices were imaged by AFM after the measurements to confirm that one and only one lysozyme was attached to the exposed SWNT channel.

A-6. Electrical measurements.

To perform high-bandwidth electrical measurements, lysozyme SWNT devices were inserted into a home-built microfluidic flow cell. First, each device was wirebonded to a ceramic chip carrier and then plugged into a 44-pin receptacle. Next, a patterned PDMS gasket was aligned over the SWNT chip, placing a 100-μm wide microfluidic channel directly over the exposed region of the SWNT FET. Clamping the gasket in place confined liquid to the desired channel and isolated from the wirebonds and contact pads.

The drain electrode was biased at 100 mV and the back gate electrode was grounded. Source-drain current $I(t)$ was measured using a FEMTO DLPCA-200 low noise preamplifer operating at 10^8 V/A gain and with a 1.8 μs rise time. This signal was digitized at 600 kHz and stored for later analysis.

After confirming electrical connectivity of the SWNT FET device, PBS was flushed into the microfluidic channel. Fluid inlets and outlets contained a combination of Pt counter electrodes, Ag/AgCl reference electrodes, and Pt pseudo-references, each of which were controlled and monitored using National Instruments data acquisition hardware (PCI-6281) and LabVIEW. Once the PBS or other fluid was in direct contact with the exposed SWNT channel, the device could be electrostatically gated by varying the Pt counter electrode. During measurements, the potential between the SWNT source electrode and the Ag/AgCl reference electrode was typically held at -0.6 or -0.7 V, a modest potential that left the p-type SWNT channel in the same doping state it would normally have in air .

In every experiment, $I(t)$ data were collected in PBS to confirm that the FET had a steady and featureless baseline current. Satisfactory devices exhibited DC resistances of 0.5 to 5.0 MΩ with no $I(t)$ features outside the 1/f noise spectrum that is normal for SWNTs. Data was collected for 600 s in PBS immediately before the introduction of peptidoglycan, and then for at least 600 s after flushing 2 mL of peptidoglycan solution through the fluid cell. At the conclusion of experiments, $I(t)$ was rechecked after flushing the peptidoglycan with 2 mL of PBS. No data was collected during fluid exchanges or flushing of the cell. In this operating limit of small, DC potentials, we assume that the SWNT FET is a passive transducer of lysozyme's activity. A previous study (*6*) showed that the $I(t)$ signals studied here are generated by these two sidechains, K83 and R119, located close to the SWNT attachment but far from lysozyme's catalytically active site. In the presence of thermal fluctuations and ionic screening, we do not believe any consequential back-action propagates from a DC-biased SWNT, through these sidechains, and back to the active site.

B. Data Analysis

SWNT FETs exhibit 1/f noise that is most significant at low frequencies. In this work, raw data was analyzed by first passing it through a 10 Hz highpass filter. After filtering, a two-peak fitting was performed on histograms of 1-second data sets to estimate the second-by-second average position of I(t) for open and closed conformations. Combining the highpass filtering with this peak-finding routine enhanced the accurate identification of events in I(t) without requiring adaptive or more aggressive filters that introduce artifacts.

After filtering, transition counting software determined and stored the absolute timestamp for every upward and downward transition in I(t). As in previous work, closure events that

lasted for fewer than 10 data points (τ_{closed} < 17 us) were rejected for additional analysis because these events could not be distinguished from extraneous noise. Subsequent analysis determined the durations $\tau_{closing}$ and $\tau_{opening}$ using a 20-80% threshold as described in the text. Each transition was categorized as continuous or discontinuous by comparing the average slope dI/dt to the maximum and minimum slopes of the smoothed data.

All analysis was performed using standard functions in LabVIEW.

C. Examples of lysozyme opening and closing transitions

Figure S1 provides additional examples of lysozyme closing events that supplement the example shown in Figure 2a (inset). Each example includes the 20-80% transition duration (red) as calculated in LabVIEW signal processing software.

The example transition in Figure S1(a) lasted for only 3 data points (~5 μs). We considered such events to be at or below the limit of our experimental resolution. The distributions plotted in Figure 2 use a histogram bin width of 30 μs so that fast events such as this one were combined with events that were resolved with much more certainty. The example transition in Figure S1(b) illustrates a 30 μs event that falls in the second bin of the histogram. The example transition in Figure S1(c) illustrates an event from the fourth bin of the histogram. Together, events like these three constitute over 90% of the total distribution of possible durations.

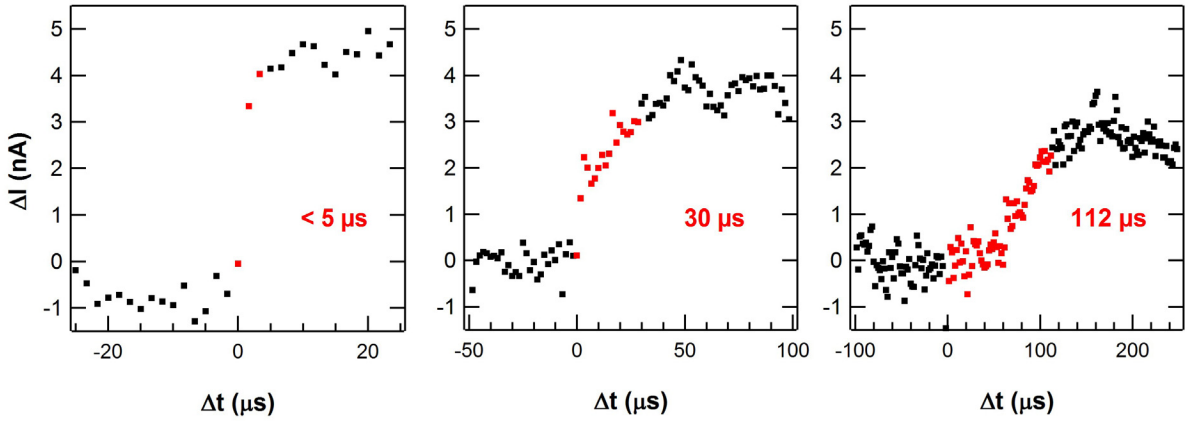

Figure S1. Three examples of continuous $\tau_{closing}$ events.

Figure S2 provides complementary examples of lysozyme opening events, supplementing the example shown in Figure 2b (inset). Each example again includes the 20-80% transition duration (red).

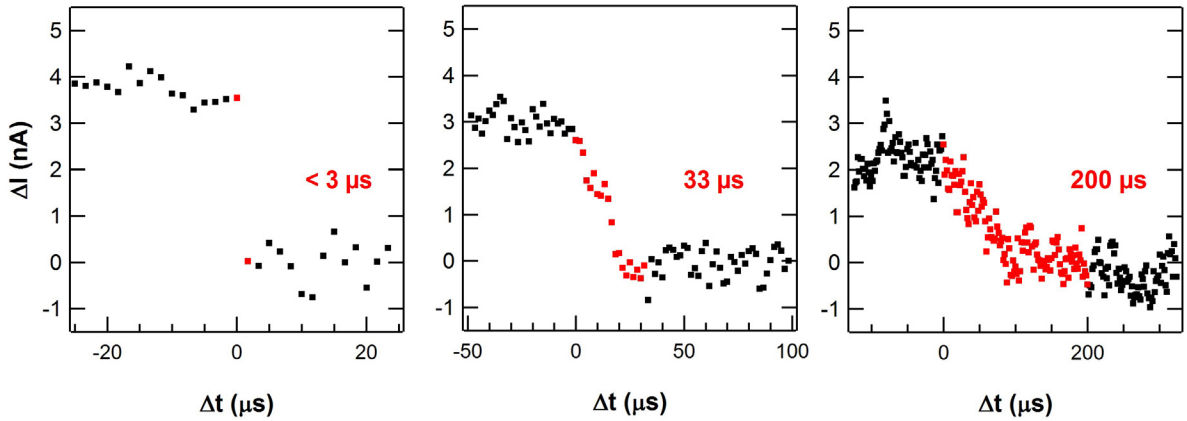

Figure S2. Three examples of continuous $\tau_{opening}$ events.

About 10% of all transition trajectories contained a single pause during the transition, leading to an intermediate plateau in $I(t)$ and a lengthened total duration. Figures S3 and S4 provide examples of closing and opening transitions, respectively, that contained such pauses.

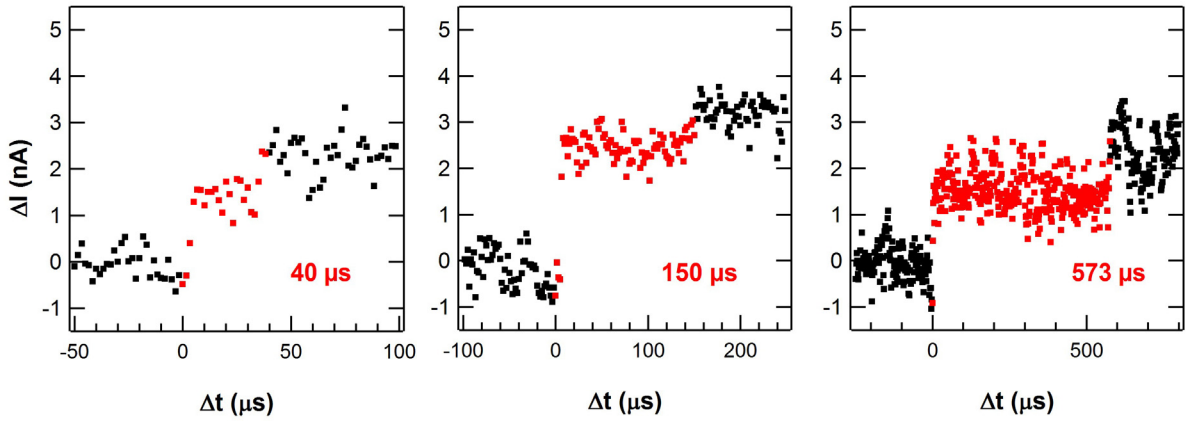

Figure. S3. Examples of lysozyme closing transitions interrupted by a pause.

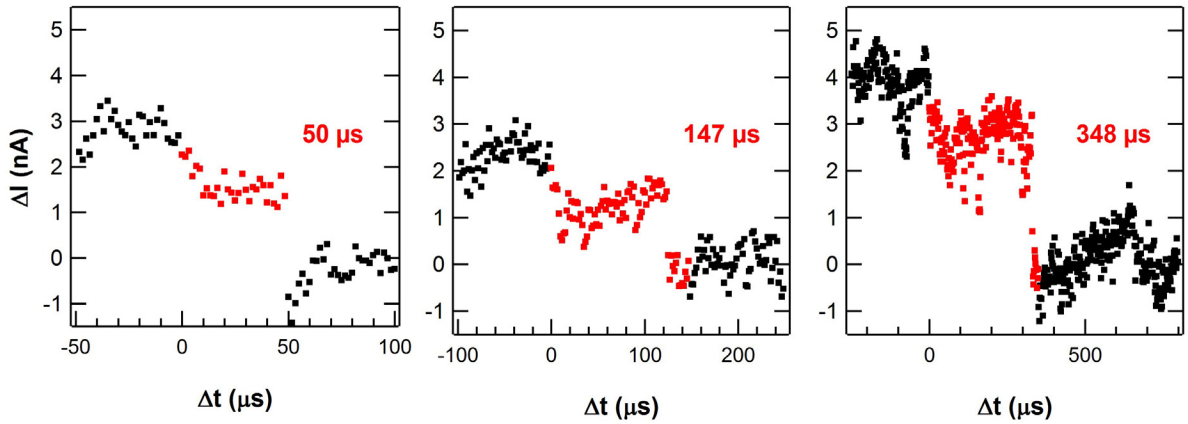

Figure. S4. Examples of lysozyme opening transitions interrupted by a pause.

D. Examples of fast electronic events

Two-level noise in a SWNT device can be caused by charge traps in the SiO_2 substrate underlying the SWNT or by oxidative damage to the SWNT sidewall (*7, 8*).

Fig. S5a shows an example of two-level switching for a SWNT damaged by partial sidewall oxidation and measured in PBS buffer. Depending on the bias conditions, the amplitude of such switching could have a signal-to-noise ratio comparable to the signals generated by lysozyme. However, a comparative analysis of two-level noise in both cases shows that only lysozyme produces fluctuations with the longer durations described in Figs. 2 and 3 and interpreted as the enzyme's mechanical motions. Two-level noise generated by SiO_2 traps or sidewall damage always exhibited abrupt transitions lasting for only a single data point (Figs. S5b and S5c). These abrupt transitions further demonstrate that the intrinsic response of the system comprising the SWNT transistor, the associated electronics, and the surrounding electrolyte was shorter than the 2 μs resolution of the current apparatus. The charge trapping mechanism is understood to have a negligible duration compared to this resolution.

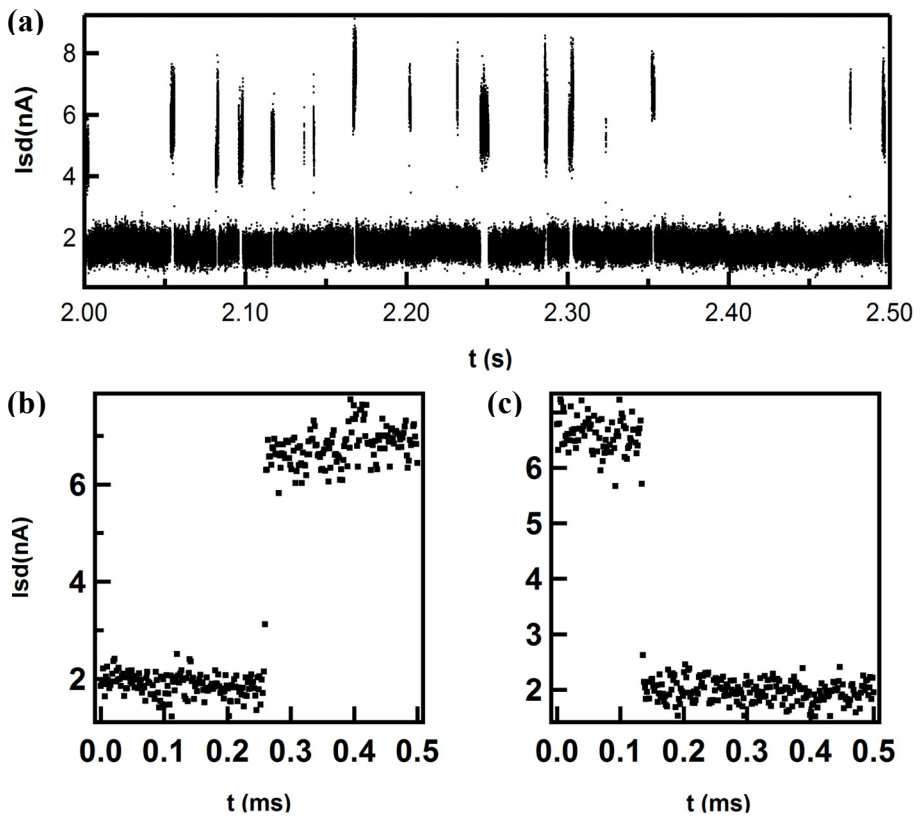

Figure. S5. (a) A representative series of stochastic two-level noise in a SWNT transistor that had been covalently damaged by sidewall oxidation. Example rising transition (b) and falling transition (c).

References

1. Zhou, R. Q., Chen, S. G., and Recsei, P. (1988) A dye release assay for determination of lysostaphin activity, *Anal. Biochem. 171*, 141-144.

2. An, L., Owens, J. M., McNeil, L. E., and Liu, J. (2002) Synthesis of nearly uniform single-walled carbon nanotubes using identical metal-containing molecular nanoclusters as catalysts, *J. Am. Chem. Soc. 124*, 13688-13689.
3. Goldsmith, B. R., Coroneus, J. G., Khalap, V. R., Kane, A. A., Weiss, G. A., and Collins, P. G. (2007) Conductance-Controlled Point Functionalization of Single-Walled Carbon Nanotubes, *Science 315*, 77-81.
4. Choi, Y., Moody, I. S., Sims, P. C., Hunt, S. R., Corso, B. L., Weiss, G. A., and Collins, P. G. (2012) Single-Molecule Lysozyme Dynamics Monitored by an Electronic Circuit, *Science 335*, 319-324
5. Chen, R. J., Zhan, Y. G., Wang, D. W., and Dai, H. J. (2001) Noncovalent sidewall functionalization of single-walled carbon nanotubes for protein immobilization, *J. Am. Chem. Soc. 123*, 3838-3839.
6. Choi, Y., Olsen, T. J., Sims, P. C., Moody, I. S., Corso, B. L., Dang, M. N., Weiss, G. A., and Collins, P. G. (2013) Dissecting Single-Molecule Signal Transduction in Carbon Nanotube Circuits with Protein Engineering, *Nano Lett. 13*, 625-631.
7. Fei, L., Wang, K. L., Daihua, Z., and Chongwu, Z. (2006) Random telegraph signals and noise behaviors in carbon nanotube transistors, *Appl. Phys. Lett. 89*, 243101-243101-243103.
8. Lin, Y.-M., Appenzeller, J., Knoch, J., Chen, Z., and Avouris, P. (2006) Low-frequency current fluctuations in individual semiconducting single-wall carbon nanotubes, *Nano Lett. 6*, 930-936.